

Magnetic Performance of (Nd,Ce)-Fe-B-type Die-upset Hybrid Magnet Composed of Melt-spun and HDDR-treated Materials

Dagus R. Djuanda^{1,2}, M. S. Kang¹, H. W. Kwon^{1*}, D. H. Kim³, J. G. Lee⁴, and H. J. Kim⁵

¹Pukyong National University, Busan 48513, Republic of Korea

²Metal Industries Development Center, Bandung 40135, Indonesia

³Star-group Ind. Co., Daegu City 42714, Republic of Korea

⁴Korea Institute of Materials Science, Changwon 51508, Republic of Korea

⁵Korea Institute of Industrial Technology, Cheonan 31056, Republic of Korea

(Received 5 September 2019, Received in final form 9 December 2019, Accepted 9 December 2019)

Ce-containing (Nd,Ce)-Fe-B-type hybrid magnet was fabricated by die-upset technique using two different types of materials: Ce-substituted $(\text{Nd}_{0.55}\text{Ce}_{0.45})_{15}\text{Fe}_{72.2}\text{Co}_{6.6}\text{Ga}_{0.6}\text{B}_{5.6}$ HDDR powder and melt-spun $\text{Nd}_{13.6}\text{Fe}_{73.6}\text{Co}_{6.6}\text{Ga}_{0.6}\text{B}_{5.6}$ flakes. Magnetic performance of the hybrid magnet was superior to that of the single alloy magnet when they had identical overall composition: $iH_c = 6.8$ kOe, $M_r = 10.6$ kG, and $(\text{BH})_{\text{max}} = 19.8$ MGOe for the Ce-containing hybrid magnet and $iH_c = 3.9$ kOe, $M_r = 9.8$ kG, and $(\text{BH})_{\text{max}} = 11.6$ MGOe for the magnet from the single alloy HDDR powder. Die-upset hybrid magnet consisting of two constituent materials showed smooth and single-material-like demagnetization behavior, and this was attributed to the exchange interaction between neighbouring grains in the magnet.

Keywords : Nd-Fe-B magnet, Ce-substitution, hybrid magnet, die-upset magnet

1. Introduction

R-Fe-B-type (R = rare-earth, mostly Nd, Pr) magnet has been widely used in a variety of applications because of its superior magnetic performance. High performance of the magnet derives from excellent intrinsic hard properties of $\text{R}_2\text{Fe}_{14}\text{B}$ -type main magnetic phase. In the main magnetic phase, rare-earth element component plays a key role, albeit its content is small, in achieving hard magnetic property: High magnetocrystalline anisotropy (MCA) of the $\text{R}_2\text{Fe}_{14}\text{B}$ -type compound, which is one of the essential intrinsic properties required for being a good hard magnetic compound, originates mostly from the rare-earth atoms. The rare-earth metals, in particular, light rare earths such as Nd, Pr and Ce, are mostly refined from rare-earth ores of Bastnasite and Monazite. In point of fact, the most abundant rare earth element in those ores is cerium: content of Ce-oxide is typically more than three times as much as that of Nd-oxide or Pr-oxide. Although the abundant Ce has wide range of applications, such as

for batteries and phosphor, supply of Ce far exceeds demand in market. Ce is considered to be the most abundant element in the rare earth family, so Ce fetches much more cheap price than Nd and Pr. It would be preferable, therefore, if the more abundant and cheaper Ce could be used as rare-earth part of the R-Fe-B-type magnet. $\text{Ce}_2\text{Fe}_{14}\text{B}$ -type compound, however, has disappointingly poor intrinsic hard magnetic properties, thus being not a good fit as base compound for permanent magnet [1-4]. Instead, a growing body of research has shown that Ce can be used as substituent for Nd in the Nd-Fe-B-type magnet with the intention of achieving balanced usage of raw materials and lowering material cost [5-11]. In this study, we investigated magnetic performance of the Ce-containing Nd-Fe-B-type die-upset hybrid magnet composed of melt-spun and HDDR-treated materials, intending to find a way for improving magnetic performance of the Ce-containing Nd-Fe-B-type magnet.

2. Experimentals

(Nd,Ce)-Fe-B-type die-upset hybrid magnet was fabricated by die-upset technique using two different types of materials: lab-prepared Ce-substituted $(\text{Nd}_{0.55}\text{Ce}_{0.45})_{15}\text{Fe}_{72.2}$ -

©The Korean Magnetism Society. All rights reserved.

*Corresponding author: Tel: +82-51-629-6353

Fax: +82-51-629-6353, e-mail: hwwkwon@pknu.ac.kr

$\text{Co}_{0.6}\text{Ga}_{0.6}\text{B}_{5.6}$ isotropic HDDR powder (particle size: 100-150 nm) was mixed with commercially available melt-spun $\text{Nd}_{13.6}\text{Fe}_{73.6}\text{Co}_{0.6}\text{Ga}_{0.6}\text{B}_{5.6}$ flakes (MQU-F, flake size: 150-200 nm). HDDR powder and melt-spun flakes are typical materials for fabrication of Nd-Fe-B-type die-upset magnet having good grain texture. Mixture of the HDDR powder and melt-spun flakes was hot-pressed at 670 °C and then die-upset at 735 °C with 75 % thick reduction. Magnetic characterization of the materials was performed using a vibrating sample magnetometer (VSM). Prior to magnetic measurement, samples were fully magnetized beforehand using 5 Tesla pulsing field. Magnetic measurement for the die-upset magnet was performed along pressing direction of the die-upsetting unless stated otherwise, which is the easy magnetization direction. Microstructure characterization and element distribution analysis were performed by electron probe microanalysis (EPMA) and scanning electron microscope (SEM) equipped with energy dispersive X-ray analysis (EDX).

3. Results and Discussion

Fig. 1 shows demagnetization curves showing magnetic performance of the Ce-substituted $(\text{Nd}_{0.55}\text{Ce}_{0.45})_{15}\text{Fe}_{72.2}\text{Co}_{0.6}\text{Ga}_{0.6}\text{B}_{5.6}$ HDDR powder and melt-spun $\text{Nd}_{13.6}\text{Fe}_{73.6}\text{Co}_{0.6}\text{Ga}_{0.6}\text{B}_{5.6}$ flake (MQU-F).

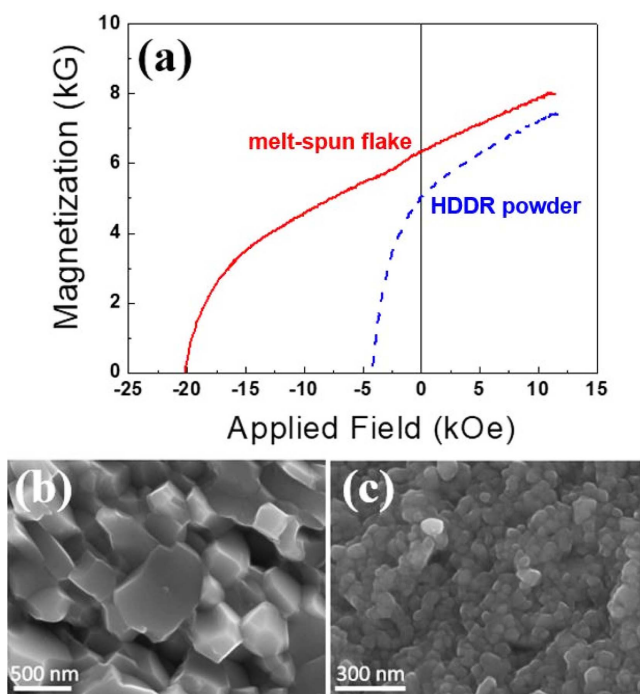


Fig. 1. (Color online) (a) Demagnetization curves of the HDDR-treated $(\text{Nd}_{0.55}\text{Ce}_{0.45})_{15}\text{Fe}_{72.2}\text{Co}_{0.6}\text{Ga}_{0.6}\text{B}_{5.6}$ powder and melt-spun $\text{Nd}_{13.6}\text{Fe}_{73.6}\text{Co}_{0.6}\text{Ga}_{0.6}\text{B}_{5.6}$ flake (MQU-F). Grain structure of (b) the HDDR-treated powder and (c) the melt-spun flake.

$\text{Co}_{0.6}\text{Ga}_{0.6}\text{B}_{5.6}$ flakes (MQU-F) used as starting materials for fabrication of the hybrid die-upset magnet. Feature of the starting materials is that they have markedly different intrinsic coercivity: MQU-F has much higher coercivity with respect to the Ce-substituted HDDR powder. High coercivity MQU-F was added to the Ce-substituted HDDR powder with the intention of enhancing magnetic performance, in particular, coercivity, of the Ce-containing Nd-Fe-B-type magnet. Markedly lower coercivity of the Ce-substituted HDDR powder was, needless to say, due largely to reduction of anisotropy field of the $\text{Nd}_2\text{Fe}_{14}\text{B}$ -type phase by substitution of Nd by Ce. As anisotropy field of the $\text{Ce}_2\text{Fe}_{14}\text{B}$ -type phase is much lower than that of the $\text{Nd}_2\text{Fe}_{14}\text{B}$ -type phase [1-4], substitution of Nd in $\text{Nd}_2\text{Fe}_{14}\text{B}$ -type phase by Ce reduces anisotropy field of the Ce-substituted HDDR powder, leading to lower coercivity. Another possible explanation for markedly lower coercivity of the Ce-substituted HDDR powder maybe coarser grain structure with respect to that in MQU-F. As can be seen in Fig. 1, grain structure in the HDDR-treated powder was noticeably larger than that in the melt-spun material, thus leading to lower coercivity. Fig. 2 shows variations of magnetic performance of the die-upset hybrid magnet with varying mixing ratio of Ce-substituted HDDR powder and MQU-F flake. Magnetic performance of the hybrid magnet improved with increasing addition of MQU-F. Profound coercivity increase of the hybrid magnet with increasing addition of high coercivity MQU-F material was achieved and this was attributed to increase of interaction between the two hard magnetic parts in the hybrid magnet. Remanence variation also showed steady increase with increasing addition of MQU-F. As the MQU-F material had greater remanence

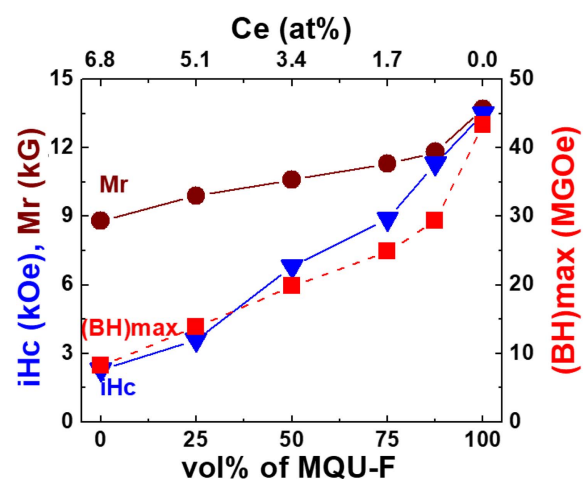


Fig. 2. (Color online) Variation of magnetic performance of the die-upset magnet with varying mixing ratio of the HDDR powder and melt-spun flake (MQU-F).

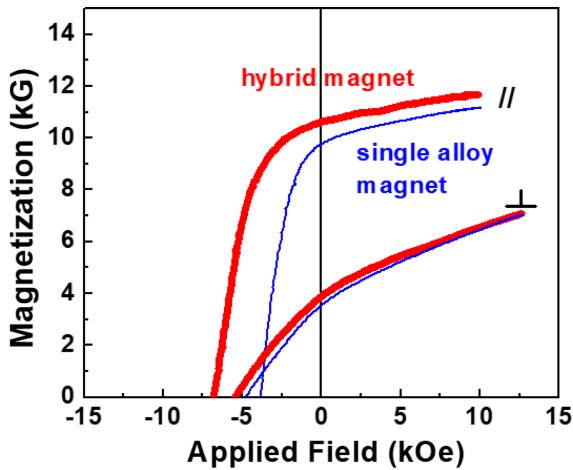


Fig. 3. (Color online) Demagnetization curves of the die-upset hybrid magnet consisting of 50 vol.% MQU-F and 50 vol.% HDDR and the die-upset single alloy magnet from only HDDR powder. These two magnets have identical overall composition ($\text{Nd}_{10.9}\text{Ce}_{3.4}\text{Fe}_{72.9}\text{Co}_{6.6}\text{Ga}_{0.6}\text{B}_{5.6}$).

with respect to the HDDR-treated material, the hybrid magnet with larger addition of MQU-F had higher remanence, accordingly. Additional contributory factor

for the remanence increase with increasing addition of MQU-F was the improved texture developed in the hybrid magnet with larger addition of MQU-F. It has been known that $\text{Nd}_2\text{Fe}_{14}\text{B}$ -type grains in a melt-spun flake and HDDR-treated Nd-Fe-B-type alloys are known to be aligned to form texture when they are deformed at an elevated temperature, and texture development in melt-spun flake is far better with respect to HDDR-treated alloy [12-16]. Therefore, overall texture in the hybrid magnet was probably controlled largely by the texture formed in the MQU-F part. Thus, overall texture had been better developed in the hybrid magnet with larger addition of MQU-F, leading to higher remanence of the hybrid magnet. We were keenly interested in comparison of magnetic performance of the hybrid magnet and single alloy magnet having identical overall composition. First, another HDDR powder, which has identical composition ($\text{Nd}_{10.9}\text{Ce}_{3.4}\text{Fe}_{72.9}\text{Co}_{6.6}\text{Ga}_{0.6}\text{B}_{5.6}$) with overall composition of the hybrid magnet with 50 vol.% starting MQU-F and 50 vol.% starting HDDR powder, was prepared. Single alloy die-upset magnet was prepared using this HDDR powder. As can be seen in Fig. 3, overall magnetic performance of the Ce-containing hybrid magnet ($H_c =$

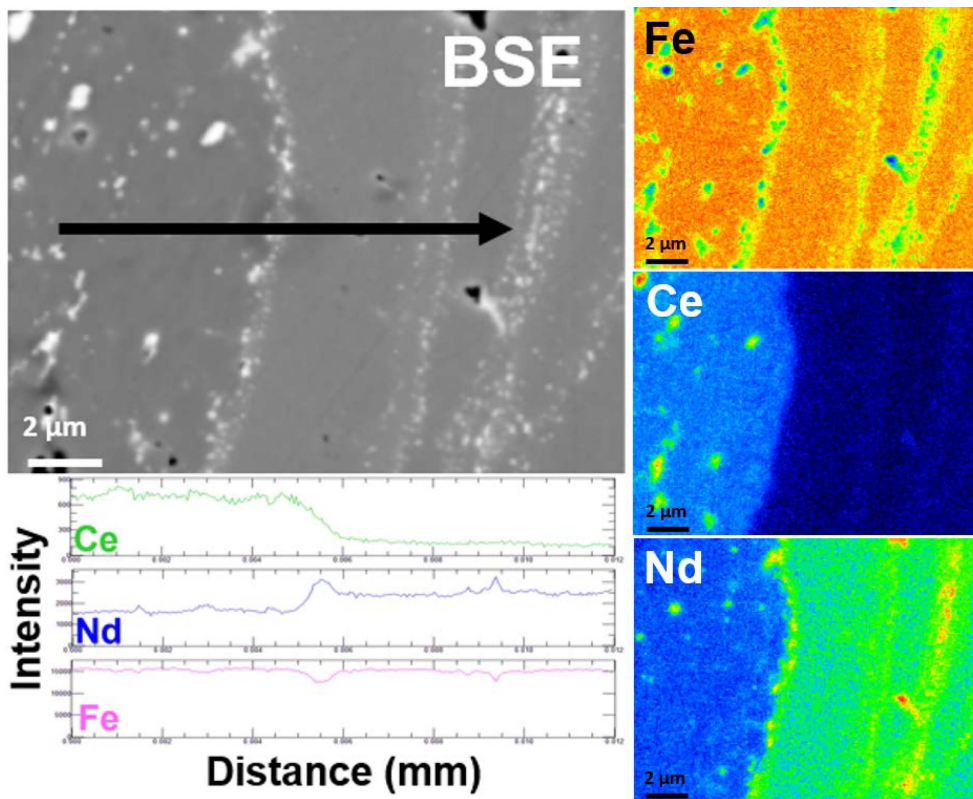


Fig. 4. (Color online) EPMA observation showing distribution of the elements in the hybrid magnet with 50 vol.% MQU-F and 50 vol.% HDDR material.

6.8 kOe, $M_r = 10.6$ kG, and $(BH)_{\max} = 19.8$ MGOe) was much superior to that ($iH_c = 3.9$ kOe, $M_r = 9.8$ kG, and $(BH)_{\max} = 11.6$ MGOe) of die-upset magnet from the single alloy HDDR powder. Worth remarking is that hybridization technique can be used as an effective means of preparing Ce-containing (Nd,Ce)-Fe-B-type magnet with good performance, which otherwise inevitably has low performance, in particular, low coercivity. Die-upset magnet only from melt-spun flake with composition identical with overall composition of the hybrid magnet would have better performance. We here emphasized the effectiveness of adding high coercivity material on enhancing inevitably low coercivity of the Ce-containing Nd-Fe-B-type magnet by hybridizing with high coercivity material.

Another interesting feature of the hybrid magnet, which was not to be overlooked, was that the hybrid magnet showed smooth and single-material-like demagnetization behavior as can be seen in Fig. 3. As the die-upset hybrid magnet was fabricated by swift process (dwelling time at higher temperature (> 650 °C) was approximately 3 minutes throughout whole process), two constituent materials in the hybrid magnet were not homogenized and still existed compositionally distinctive parts with absolute boundary between them as shown in Fig. 4. Despite consisting of separate constituents, the hybrid magnet showed single-material-like demagnetization curve. This indicated that fine grains not only in each constituent but also across the boundary between the two different constituent materials in the hybrid magnet were magnetically coupled strongly through inter-grain interaction. Inter-grain interaction operating in a permanent magnetic material is either the long-range magnetostatic (dipolar) interaction or the exchange coupling between the adjacent grains [17-20]. Confirming which inter-grain interaction operates dominantly in a magnetic material can be accomplished by Henkel plot [17], in which two types of remanence curves are compared: isothermal remanent magnetization (IRM) curve ($M_r(H)$) and DC demagnetization remanent magnetization (DCD) curve ($M_d(H)$). The $M_r(H)$ curve is obtained by progressively magnetizing and measuring of remanent magnetization for a thermally demagnetized sample, and the $M_d(H)$ curve is obtained by measuring the remanent magnetization after demagnetizing by progressively increasing and removing reverse field for a sample fully magnetized beforehand. Type and strength of the dominant interaction between the neighbouring grains can be addressed by the Henkel relation given below.

$$\delta M(H) = m_d(H) - [1 - 2 m_r(H)]$$

Where $m_r(H)$ and $m_d(H)$ are normalized value of $M_r(H)$ and $M_d(H)$ against $M_r(\infty)$, respectively, which is the re-

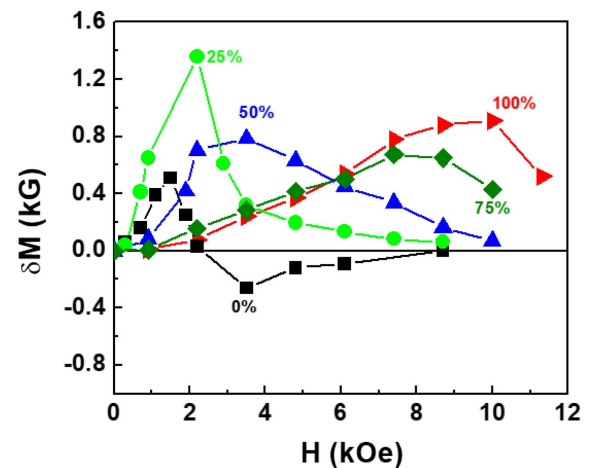


Fig. 5. (Color online) Henkel plots for revealing an inter-grain interaction for the hybrid magnets with varying addition of MQU-F material (vol.%).

manence value after saturation magnetization in forward direction. Depending on the value of $\delta M(H)$, inter-grain interaction operating dominantly in a magnetic material is addressed: Positive and negative $\delta M(H)$ curves suggest that dominant inter-grain interaction is the exchange interaction and the magnetostatic interaction, respectively. Fig. 5 shows Henkel plot obtained from the remanence curves measured parallel with pressing direction for the die-upset magnets. As can be seen, when the applied field is small, the $\delta M(H)$ curve showed positive value for all the die-upset magnets. With increasing applied field, the $\delta M(H)$ increased, and after showing peak at the field slightly lower than the coercivity, it decreased. Positive

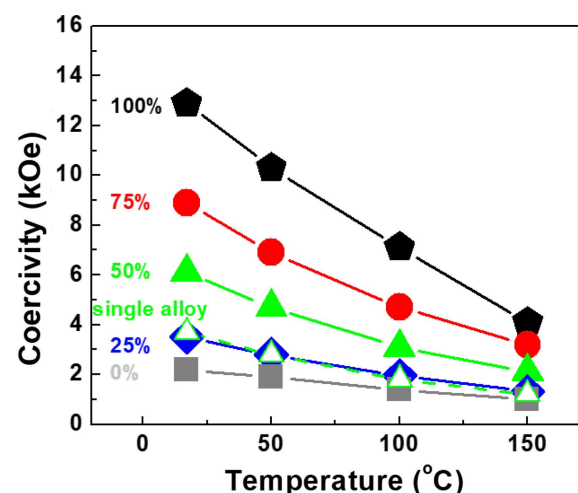


Fig. 6. (Color online) Temperature dependence of coercivity of the die-upset hybrid magnet with varying mixing ratio of MQU-F and HDDR materials. 50/50 hybrid magnet and single alloy magnet have identical composition ($\text{Nd}_{10.9}\text{Ce}_{3.4}\text{Fe}_{72.9}\text{-Co}_{6.6}\text{Ga}_{0.6}\text{B}_{5.6}$).

Table 1. Temperature coefficients of coercivity (β) of the hybrid magnets with varying addition of MQU-F material.

MQU-F (vol.%)	100	75	50	25	0	Single alloy*
β (%/K)	–0.513	–0.482	–0.493	–0.473	–0.413	–0.508

*Single alloy magnet has identical composition (Nd_{10.9}Ce_{3.4}Fe_{72.9}Co_{6.6}Ga_{0.6}B_{5.6}) with that of 50/50 hybrid magnet.

value of $\delta M(H)$ curve up to the field strength over coercivity suggests that dominant inter-grain interaction operating in the hybrid magnets is exchange-coupling. Obviously, the smooth and single-material-like demagnetization behavior of the hybrid magnet is believed to be caused by the exchange interaction between the grains not only in each constituent but also across the boundary between the two different constituents.

Fig. 6 shows temperature dependence of coercivity of the die-upset hybrid magnet with varying mixing ratio. With increasing vol.% of MQU-F material, room temperature coercivity and temperature coefficient of coercivity (β) of the hybrid magnet increased. It seems that higher temperature coefficient of coercivity of the hybrid magnet with larger vol.% of MQU-F material is contrary to our expectation. It has been commonly known that temperature coefficient of coercivity of Nd-Fe-B-type magnet is improved (decreased) with decreasing grain size [21, 22]. In the hybrid magnet, MQU-F material part has much finer grain size with respect to HDDR part. Then, better (smaller) temperature coefficient of coercivity is expected in the hybrid magnet with larger vol.% of MQU-F material. Present results seem to be the other way around, and explanation for this unexpected behavior has not been fully understood. Temperature coefficients of coercivity (β) of the hybrid magnets were presented in Table 1. It is noted that the Ce-containing hybrid magnet (50/50 mixing ratio) has more or less similar β value with that of single alloy.

4. Conclusion

Fabrication of Ce-containing Nd-Fe-B-type die-upset magnet with good magnetic performance was feasible by hybridization between (Nd,Ce)-Fe-B-type HDDR powder and Nd-Fe-B-type melt-spun flake. Magnetic performance of the hybrid magnet was superior to that of the single alloy magnet when they had identical overall composition: $iH_c = 6.8$ kOe, $M_r = 10.6$ kG, and $(BH)_{max} = 19.8$ MGOe for the Ce-containing hybrid magnet and $iH_c = 3.9$ kOe, $M_r = 9.8$ kG, and $(BH)_{max} = 11.6$ MGOe for the magnet from the single alloy HDDR powder. Despite consisting of two constituent materials being compositionally distinctive, the die-upset hybrid magnet showed smooth and single-material-like demagnetization behavior, and this

was attributed to the exchange interaction between neighbouring grains in the magnet.

Acknowledgement

The authors gratefully acknowledge that the present work was financially supported by the Technology Innovation Program from the Ministry of Trade, Industry & Energy (MOTIE, Republic of Korea) (No.10080382).

References

- [1] R. Grössinger, X. K. Sun, R. Eibler, K. H. J. Buschow, and H. R. Kirchmayr, *Le J. Phys. Colloq.* **46**, C6-221 (1985).
- [2] C. Abache and J. Oesterreicher, *J. Appl. Phys.* **60**, 3671 (1986).
- [3] J. F. Herbst, *J. Rev. Mod. Phys.* **63**, 819 (1991).
- [4] J. F. Herbst, M. S. Meyer, and F. E. Pinkerton, *J. Appl. Phys.* **111**, 07A718 (2012).
- [5] E. J. Skoug, M. S. Meyer, F. E. Pinkerton, M. M. Tessema, D. Haddad, and J. F. Herbst, *J. Alloys Compd.* **574**, 552 (2013).
- [6] A. Alam, M. Khan, R. W. Mccallum, and D. D. Johnson, *Appl. Phys. Lett.* **102**, 42402 (2013).
- [7] C. Yan, S. Guo, R. Chen, D. Lee, and A. Yan, *IEEE Trans. Magn.* **50**, 2102605 (2014).
- [8] A. K. Pathak, M. Khan, K. A. Gschneidner Jr., R. W. Mccallum, L. Zhou, K. Sun, K. W. Dennis, C. Zhou, F. E. Pinkerton, and M. J. Kramer, *Adv. Mater.* **27**, 2663 (2015).
- [9] Z. B. Li, B.G. Shen, M. Zhang, F. X. Hu, and J. R. Sun, *J. Alloys Compd.* **628**, 325 (2015).
- [10] A. K. Pathak, M. Khan, K. A. Gschneidner Jr., R. W. Mccallum, L. Zhou, K. Sun, and M. J. Kramer, *Acta Mater.* **103**, 211 (2016).
- [11] Z. B. Li, M. Zhang, B. G. Shen, F. X. Hu, and J. R. Sun, *Mater. Lett.* **172**, 102 (2016).
- [12] J. F. Herbst and J. J. Croat, *J. Magn. Magn. Mater.* **100**, 57, (1991).
- [13] P. J. McGuinness, C. Short, A. F. Wilson, and I. R. Harris, *J. Alloys Compounds* **184**, 243 (1992).
- [14] A. Kirchner, W. Grünberger, O. Gutfleisch, V. Neu, K.-H. Müller, and L. Schultz, *J. Phys. D, Appl. Phys.* **31**, 1660 (1998).
- [15] R. Gopalan H. Sepehri-Amin, K. Suresh, T. Ohkubo, K. Hono T. Nishiuchi, N. Nozawa, and S. Hirosawa, *Scripta*

- Mater. **61**, 978 (2009).
- [16] J. G. Yoo, H. R. Cha, J. Y. Jung, Y. K. Kim, Y. K. Baek, D. Y. Lee, H. W. Kwon, and J. G. Lee, IEEE Trans. Magn. **54**, 2102305 (2018).
- [17] E. P. Wohlfarth, J. Appl. Phys. **29**, 595 (1958).
- [18] E. F. Kneller and R. Hawig, IEEE Trans. Magn. **27**, 3588 (1991).
- [19] R. Skomski and J. M. D. Coey, Phys. Rev. B **48**, 1581 (1993).
- [20] L. Folks, R. Street, and R. Woodward, J. Appl. Phys. **75**, 6271 (1994).
- [21] Y. Une and M. Sagawa: The 21st Int. Workshop on Rare-Earth Permanent Magnets and Their Applications, Bled, Slovenia (2010).
- [22] H. Sepehri-Amin, Y. Une, T. Ohkubo, K. Hono, and M. Sagawa, Scr. Mater. **65**, 396 (2011).